

Fracture Studies in Rubber-Modified Polymers. II. Experimental Results: Fracture Surface Work of Rubber-Modified Acrylics

T. KOBAYASHI* and L. J. BROUTMAN, *Department of Metallurgical and Materials Engineering, Illinois Institute of Technology, Chicago, Illinois 60616*

Synopsis

With the use of a sandwich-tapered double-cantilever beam cleavage specimen (described in part I of this series), the fracture surface work of several commercial and experimental acrylic multipolymers has been measured as a function of crack velocity and rubber content. The plots of fracture surface work versus crack velocity clearly exhibit the effects of rate (crack velocity) and rubber concentration on fracture behavior. Specifically, the fracture surface work of specimens with seven different rubber contents has been determined over a crack velocity range from 10^{-5} meters/sec to approximately 10 meters/sec. For each material, distinct maxima occur in the curves of fracture surface work versus crack velocity. The significance of these observations is discussed.

INTRODUCTION

Rubber-modified polymers have been developed to improve the impact resistance of brittle glassy polymers. The characterization of the impact and fracture resistance of these materials, however, has been a difficult problem. One of the main reasons for this difficulty is that well-established fracture toughness testing methods cannot be utilized because of the high ductility of the polymer. The Charpy and Izod impact tests are the most frequently used testing methods for characterizing the toughness of the ductile polymers. These testing methods are, however, quite restricted in testing speed and, in fact, only evaluate the fracture resistance at one impact velocity. It is also difficult to analyze the measured value of impact energy because it is the sum of the energy required to initiate and to propagate a crack. In many polymeric materials, these two energies are quite different in magnitude and, furthermore, the energy required to propagate the crack is strongly dependent on crack velocity. It is, therefore, important to develop a testing method which can be used to characterize the fracture toughness or fracture surface work (energy required to create a unit area of fracture surface) as a function of crack velocity. By characterizing fracture surface work as a function of crack velocity, one may be able to better explain the exact role of the rubber phase in toughening mechanisms. In part I of this paper, a new sandwich-tapered double-cantilever beam

* Present address: Department of Mechanical Engineering, University of Maryland, College Park, Maryland.

cleavage specimen was discussed. With this specimen, a crack can be propagated through tough and ductile materials in a controlled manner, and thus the fracture surface work can be determined as a function of crack velocity. In this part, the results obtained from several commercial and experimental rubber-modified acrylics and the analysis of these results will be discussed.

TEST MATERIALS AND SPECIMEN PREPARATION

The materials investigated in this study are commercial acrylic multipolymers, XT-500* and XT-375 (trade names American Cyanamid Co.), and experimental acrylic multipolymers (these polymers were supplied to us as injection-molded plates by the U.S. Army Materials and Mechanics Research Center) with seven different rubber content levels (0, 1, 4, 7, 10, 13, and 16% rubber). In order to identify each experimental acrylic multipolymer, an abbreviation such as AMP 10 will be used to designate, for example, a 10% rubber content polymer. The variation in modulus and yield strength as a function of rubber content for the experimental acrylic multipolymers are summarized in Figure 1.¹ The mechanical properties for XT-500 and XT-375 are summarized in Table I. Most of the materials used were obtained in the form of injection-molded plates (10 in. \times 10 in. \times 0.1 in.). The XT-500 polymer was obtained as extruded sheet with thicknesses of 0.10 in. and 0.06 in. All injection-molded plates were found to have high residual stresses. The following annealing process was therefore applied to the material in order to relieve the residual stresses: (1) the plates were subjected to 100°C temperature for 10 hr; (2) the temperature was lowered to room temperature at a cooling rate of 5°C per 10 minutes.

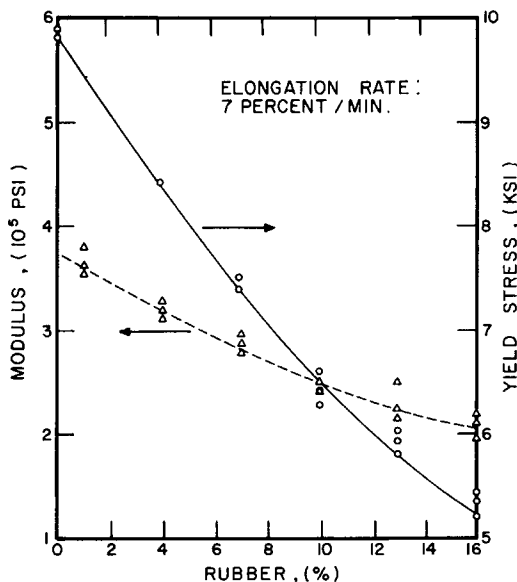


Fig. 1. Tensile modulus and yield stress of rubber-modified acrylics (Ref. 1).

TABLE I
Typical Properties of XT-Polymers

Property	ASTM Method	XT-500	XT-375
Izod impact strength, ft lb/in. of notch (1/4 in. bar)	D-256-56		
73°F		3.0	2.0
32°F		2.3	—
-40°F		1.6	1.2
Tensile strength, psi	D-638-60T	6000	7000
Tensile elongation, %	D-638-60T		
at yield		3.6	3.6
at break		40	28
Flexural strength, psi	D-790-59T	9500	11000
Flexural modulus, psi	D-790-59T	300000	350000
Rockwell hardness	D-785-60T	R108	R114
		M24	M45
Deflection temperature at 264 psi, °F	D-648-56	193	194
Light transmission, %	D-307-44	87	87
Haze	D-1003-52	9	9
Specific gravity	D-792	1.09	1.10

After the annealing process, a 1/8-in.-thick Plexiglas plate was glued to each side of the rubber-modified acrylic with acrylic adhesive (PS-30, Cadillac Plastics and Chemicals Company), thus creating a sandwich structure. The adhesive was cured at a temperature of 50°C at 50 psi pressure for 4 hr. Side grooves and initial cracks were machined into the sheet with a specially designed side-groove cutting machine. While cutting the grooves, a water-soluble oil was used with a ratio of ten parts of water to one part oil and the specimen was sprayed with compressed air in order to eliminate heat generation in the cutting area. Immediately after machining the side grooves and initial crack, the specimens were washed thoroughly with water to remove the water-soluble oil. Excess water was removed with compressed air.

The next step in the specimen preparation was machining the contour of the tapered double-cantilever beam specimen and the two loading pin holes. After the specimen was machined, eight silver conductive paint lines were drawn at half-inch intervals along the crack plane for crack velocity measurements during high-speed testing. Specimen testing was done in an Instron testing machine at low cross-head rates (0.02 to 5 inches per minute) and in a servo-controlled hydraulic high speed loading machine at high cross-head rates (10 to 7000 inches per minute). In low-speed tests, crack tip positions were visually observed and marked on the load-displacement chart from which crack velocities were calculated. In high-speed tests, the conductive paint lines generated voltage drops when the crack passed and broke each line, and from the records of voltage drops versus time, crack velocities were obtained. From the load-deflection

records and crack tip position, the experimental compliance change $\partial C/\partial l$ was calculated and used to determine the fracture surface work. The fracture surface work was obtained by utilizing Irwin's definition of the critical crack extension force, which is twice the fracture surface work,

$$G_c = 2\gamma = \frac{f_c^2}{2w} \frac{\partial C}{\partial l}$$

where f_c is the applied load and w is the crack width. The procedure was discussed in detail in part 1 of this series.

EXPERIMENTAL RESULTS

Results of experiments at three different crack velocities are shown in Figures 2-4. The numbers marked on the load-deflection curves in Figures 2 and 3 represent the crack tip positions measured from the loading point (crack length) during the test. In the case of the high-speed testing, the crack tip positions are indicated by a staircase-like electrical signal record shown in Figure 4. These figures show that the load and the crack extension rate remain relatively constant; thus, the sandwich-tapered double-cantilever beam specimen is very suitable for studying the fracture surface work as a function of crack velocity.

Figure 5 summarizes the results of fracture surface work versus crack velocity for two commercial XT-polymers, XT-500 and XT-375. In order to more quantitatively study the effects of rubber concentration on the fracture surface work, the experimental rubber-modified acrylics with seven

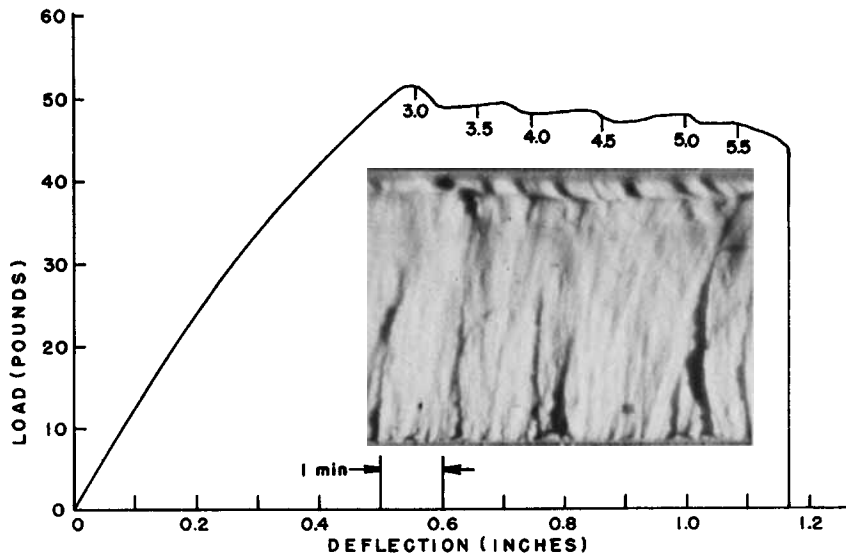


Fig. 2. Load-deflection curve and fracture surface of rubber-modified acrylic (XT-500). Cross-head rate was 0.1 in./min.

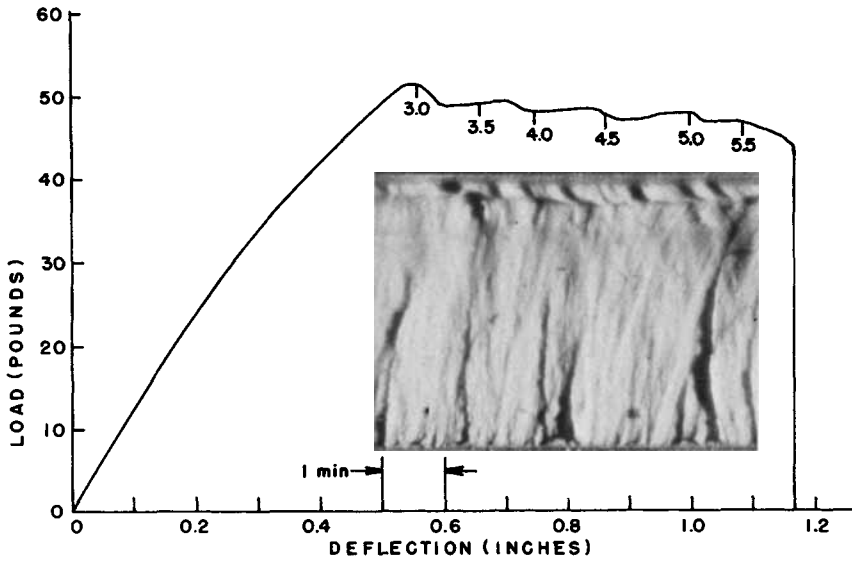


Fig. 3. Load-deflection curve and fracture surface of rubber-modified acrylic (XT-375). Cross-head rate was 1 in./min.

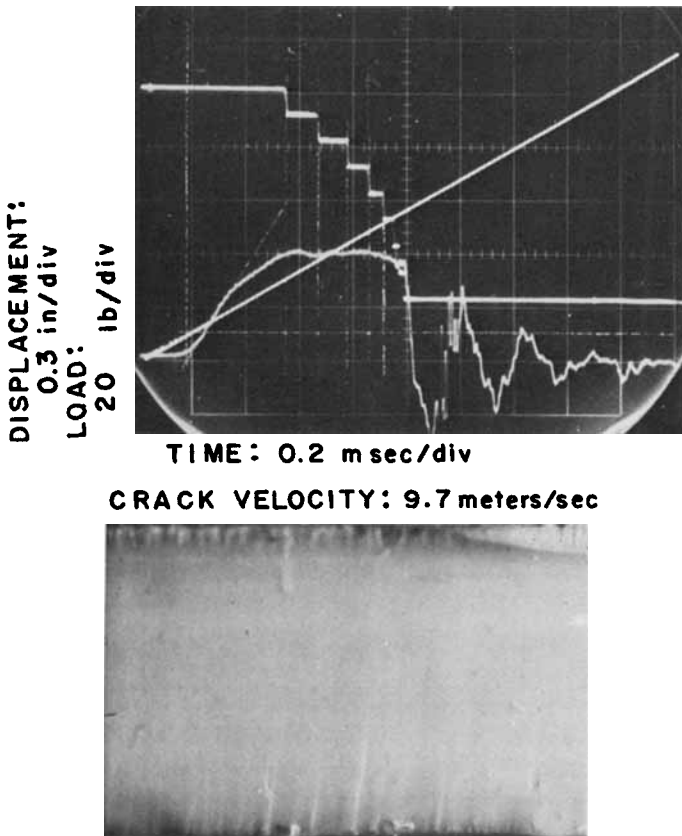


Fig. 4. Load, deflection, and crack tip position record on oscilloscope trace and fracture surface of rubber-modified acrylic (XT-375). Cross-head rate was 5143 in./min.

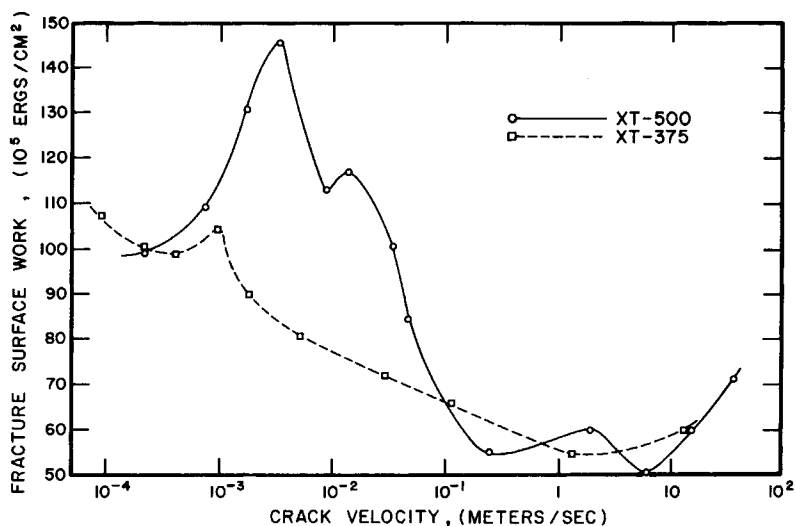


Fig. 5. Fracture surface work as a function of crack velocity for XT-375 and XT 500 polymers.

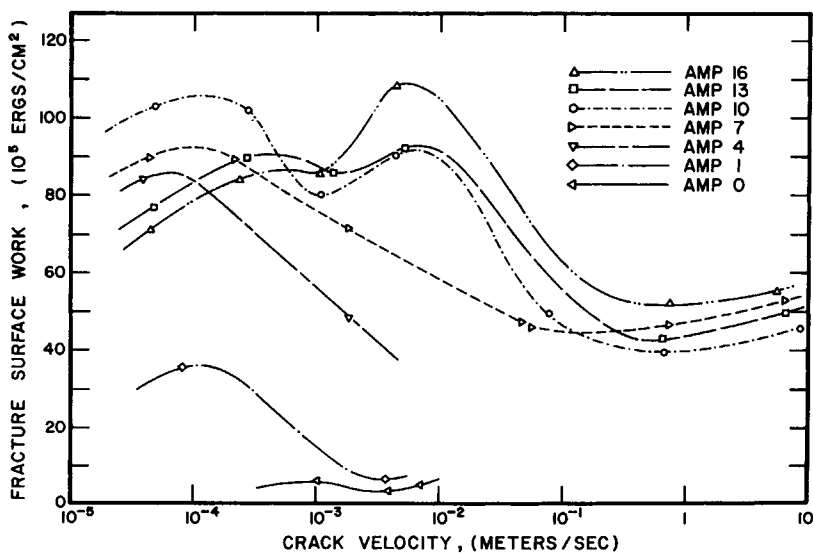
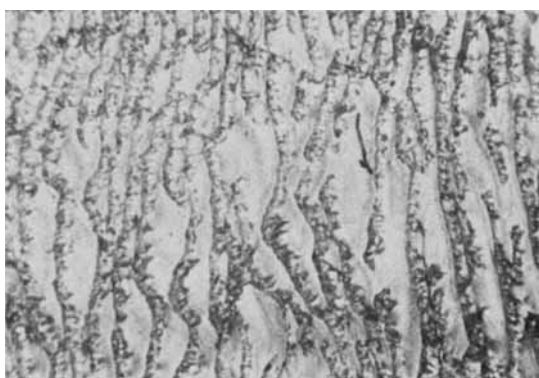


Fig. 6. Fracture surface work vs. crack velocity for acrylic multipolymers.

different rubber concentrations were studied, and the results are shown in Figure 6. The fracture surfaces at various crack velocities are shown in Figures 7-9. Stress whitening is observed for all materials except AMP 0 (no rubber) at low crack velocities. For materials with low rubber concentrations (1% and 4%), stress whitening is eliminated at moderate crack velocities and the fracture surface appearance becomes quite similar to the fracture surface appearance of the material with no rubber (AMP 0).



(a)



(b)

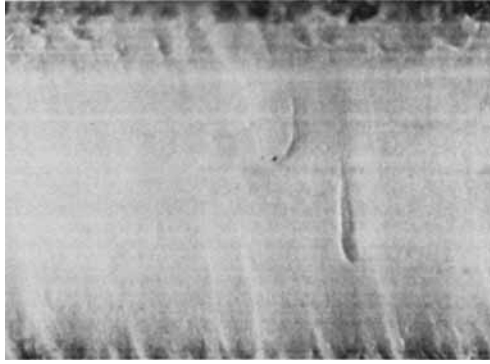
Fig. 7. Fracture surfaces of unmodified acrylics (AMPO) polymer.

DISCUSSION

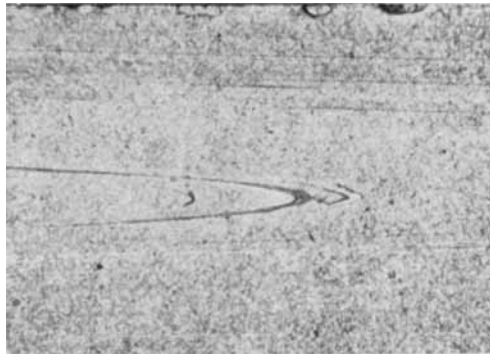
The curve of fracture surface work versus crack velocity for XT-500 (Fig. 5) shows that the fracture surface work increases as the crack velocity increases up to approximately 3.2×10^{-3} meter/sec. At approximately 3.2×10^{-3} meter/sec, the fracture surface work passes through a maximum and then starts to decrease as the crack velocity increases. Another local maximum is observed at a crack velocity of approximately 2.5×10^{-1} meter/sec. The curve of fracture surface work versus crack velocity for the XT-375 materials first decreases as the crack velocity increases, and at approximately 4.2×10^{-4} meter/sec the fracture surface work takes a local minimum. The fracture surface work starts to increase above 4.2×10^{-4} meter/sec and takes a local maximum value at approximately 10^{-3} meter/sec. Above 10^{-3} meter/sec, the fracture surface work gradually decreases as the crack velocity increases up to approximately 1.5 meters/sec. The trend of the curve suggests that another maximum may exist below the crack velocity range of 10^{-4} meter/sec. Thus, the curves

for XT-500 and XT-375 would be quite identical at low crack velocities but displaced in time.

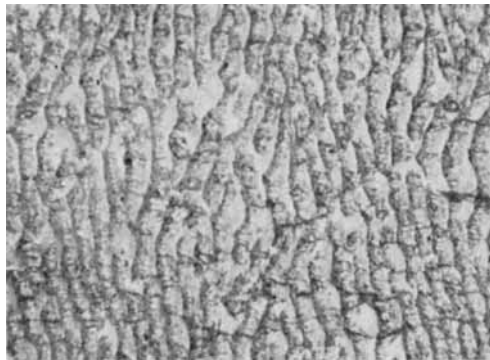
In further comparing the fracture surface work curves one can see that major differences in magnitude exist below the crack velocity of 10^{-1} me-



(a)



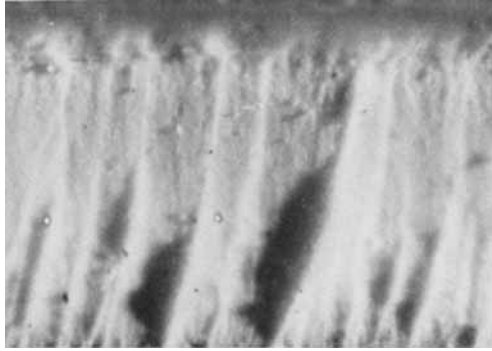
(b)



(c)

Fig. 8. Fracture surfaces of 1% rubber-modified acrylic polymer at different crack velocities.

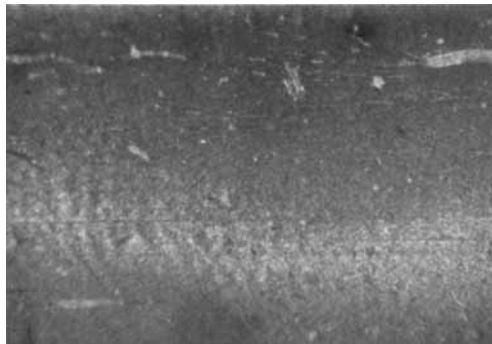
ter/sec. Above this crack velocity, the materials exhibit quite similar levels of fracture resistance although small local differences exist. If the major material difference between XT-500 and XT-375 is the rubber concentration, it can then be concluded that the difference in the curves (be-



(a)



(b)



(c)

Fig. 9. Fracture surfaces of 4% rubber-modified acrylic polymer at different crack velocities.

low the crack velocity of 10^{-1} meter/sec) is caused by the difference in rubber concentration. Thus, these curves define the range of crack velocity, i.e., rate, for which the rubber inclusion has a strong influence on the fracture process. A large value of fracture surface work at the crack velocity of 3.2×10^{-3} meter/sec, caused by the inclusion of rubber, governs the crack stability. If the fracture surface work increases as the crack velocity increases, it is necessary to increase the crack driving force to accelerate the moving crack. In other words, as the crack accelerates, the fracture resistance is increasing. For this condition, the crack propagates in a stable and continuous manner. On the other hand, when the fracture surface work decreases as the crack velocity increases, the crack propagates in an unstable manner. This is due to the crack driving force becoming higher than the fracture resistance of the material as the crack velocity increases. Therefore, in order for the crack to seek a balance between the crack driving force and the fracture resistance of the material, the crack must accelerate. The rate of decrease in fracture surface work as a function of crack velocity governs the degree of instability. If the rate of decrease is large, the crack propagation becomes highly unstable and a crack jump or stick slip mode of propagation occurs.

To characterize the material fracture performance, it is thus necessary to study the location and magnitude of the peaks on the curve of fracture surface work versus crack velocity.

The curve for XT-375 is assumed to have a peak below the crack velocity of 10^{-4} meter/sec, and the level of fracture surface work is higher than that for XT-500 in this crack velocity range. This indicates that when the crack is moving at less than 10^{-4} meter/sec, XT-375 may have a greater resistance to crack propagation than XT-500. But, under impact, if the impact energy is great enough to accelerate the crack beyond the crack velocity of 10^{-3} meter/sec, the crack propagates more easily in XT-375 than in XT-500 because the level of fracture surface work is lower for XT-375 than for XT-500 at greater velocities, and the fracture surface work is constantly decreasing beyond the crack velocity at 10^{-3} meter/sec up to 1.5 meter/sec.

At this point it is of interest to examine the meaning of the notched Izod impact test and its results. The notched Izod impact strength for XT-500 at 73°F is 3.0 ft lb per inch of notch and 2.0 ft lb per inch of notch for XT-375. Thus, XT-500 exhibits an impact strength about 1.5 times greater than the impact strength of the XT-375 material. However, the fracture surface work of XT-500 and XT-375 at high crack velocities do not show any significant difference. From the curves in Figure 5 and considering the nature of the notched Izod impact test, it is suggested that the energy obtained from the notched Izod impact test may be related to the area under the curve of fracture surface work versus crack velocity and, thus, may be strongly influenced by the fracture resistance of the material in the low crack velocity region. From this point of view, the quantity ob-

tained by the notched Izod impact test may not be a true representation of material response at high rate, although it is usually considered to be a high rate test.

From the results in Figure 6, the effect of rubber concentration on the relation between fracture surface work and crack velocity can be analyzed. The fracture surface work of the matrix polymer averages 5×10^5 ergs/cm². The inclusion of 1% rubber increases the fracture surface work approximately seven times. However, this increase in fracture surface work occurs only in the crack velocity range below 5×10^{-4} meter/sec. When the crack velocity exceeds 3×10^{-3} meter/sec, the fracture surface work reduces to the level of the material without rubber. In other words, the effect of the rubber inclusion is diminished when the crack velocity increases. The fracture surface appearance shown in Figure 8 clearly indicates this phenomena. When the crack velocity is below 5×10^{-4} meter/sec, dense stress whitening is observed on the fracture surface; however, when the crack velocity reaches 3.53×10^{-3} meter/sec, stress whitening diminishes until only numerous white points are observed on the glassy transparent fracture surface. The AMP 4 and AMP 7 materials exhibit a similar behavior for the curve of fracture surface work versus crack velocity. The fracture surface work in the low crack velocity region is large and it decreases as the crack velocity increases. However, the values of fracture surface work are raised substantially in comparison with those of AMP 0 and 1 over the entire crack velocity range investigated.

The curves of fracture surface work versus crack velocity for the materials containing over 10% rubber behave differently from those for the materials containing 1%, 4%, and 7% rubber. AMP 10, 13, and 16 exhibit a second peak on the curve of fracture surface work versus crack velocity. The fracture surface work of these materials first increases as the crack velocity increases up to approximately 2.4×10^{-4} meter/sec; then it starts to decrease. At about 10^{-3} meter/sec, the fracture surface work curves take a minimum value, and above 10^{-3} meter/sec they increase again as the crack velocity increases. The fracture surface work curves then take a peak at approximately 4×10^{-3} meter/sec. Above this crack velocity, the fracture surface work decreases as the crack velocity increases up to approximately 6.7×10^{-1} meter/sec. Then it starts to increase slightly again.

It is of great interest to study the change in magnitude of two peaks on the curves of fracture surface work versus crack velocity with respect to rubber concentration. For example, AMP 10 shows the highest first peak at a crack velocity of approximately 2.4×10^{-4} meter/sec. As the rubber concentration increases over 10%, the magnitude of the first peak decreases. This can also be seen in Figure 10 where fracture surface work is plotted versus rubber content for three crack velocities. On the other hand, the magnitude of the second peak at a crack velocity of approximately 4×10^{-3} meter/sec increases as the rubber concentration increases. AMP

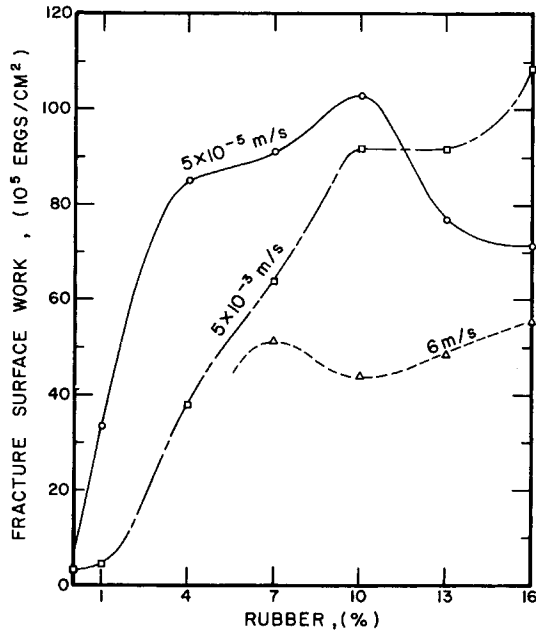


Fig. 10. Fracture surface work of acrylic multipolymers at three different crack velocities.

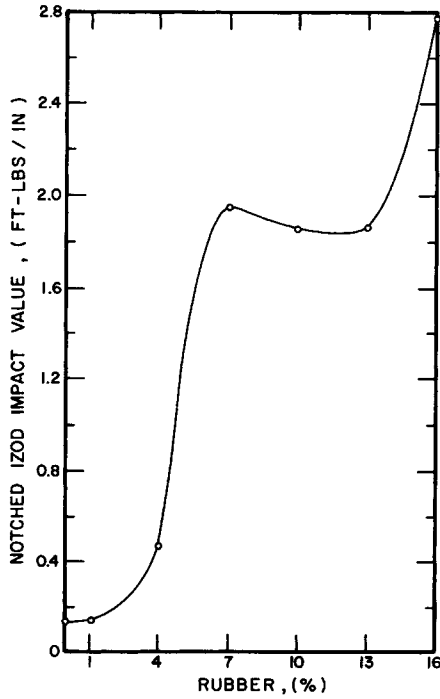


Fig. 11. Notched Izod impact strength as a function of rubber content.

16 thus exhibits the highest second peak (also see Fig. 10). The variation of these two peaks will be further discussed in the third part of this series in which the dynamic damping characteristics will be related to the observed fracture toughness behavior. At this point, one can state that it would be desirable for a material to have a high first peak and to have it occur at as high a crack velocity as possible. This would inhibit the occurrence of rapid unstable crack propagation in a situation where the crack extension force is increasing with increasing crack length.

The notched Izod impact strengths for the experimental rubber-modified acrylics at room temperature are shown in Figure 11. The results for the

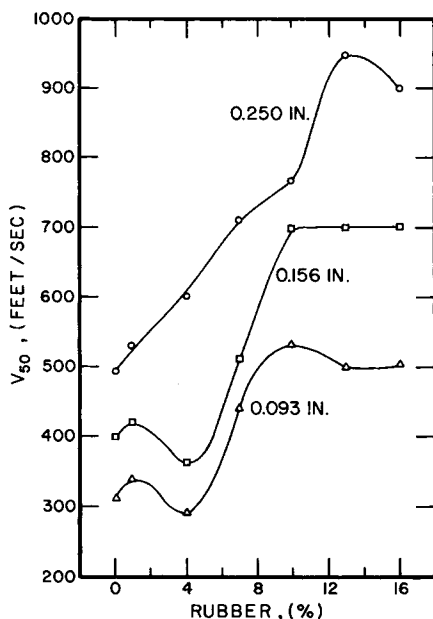


Fig. 12. V_{50} ballistic limit of rubber-modified acrylic as a function of rubber content for 17 grain 0.22 caliber fragment simulators (ref. 1).

V_{50} ballistic limits of these materials obtained by Lewis et al.¹ are shown in Figure 12. A notched Izod impact test predicts that AMP 16 would have the highest impact resistance, but the results of ballistic tests show that AMP 10 or 13 exhibits the highest resistance. These discrepancies may be better analyzed by studying the crack velocity or strain rate distribution in these tests and correlating the rate distribution to the results obtained here for fracture resistance as a function of crack velocity. It is clear from Figure 10 that, since the fracture surface work variation with rubber content is so dependent upon the crack velocity, the results from one standard test cannot be used to rate the behavior of materials in another application where loading rates may be entirely different.

CONCLUSIONS

The study of fracture surface work variation as a function of crack velocity is useful for developing an understanding of the effect of the rubber inclusion and the rubber concentration. This information should be useful to help design new materials. Furthermore, it should be useful to evaluate the significance of different impact test methods.

This study was part of a Ph.D. Thesis submitted to the Illinois Institute of Technology by Dr. Takao Kobayashi. The research was supported by the U.S. Army Materials and Mechanics Research Center under Contract No. DAAG 46-69-C-0075.

References

1. R. W. Lewis, M. W. Roylance, and G. R. Thomas, *Rubber Toughened Acrylic Polymers for Armor Applications*, AMMRC, Watertown, Mass.

Received August 20, 1972